

RESEARCH

Open Access



# *In-situ* monitoring of $^3\text{He}/^4\text{He}$ in summit gases of Kilauea Volcano (Hawaii) prior to the 2020 eruption

Gary M. McMurtry<sup>1\*</sup> and Luis A. Dasilveira<sup>2</sup>

## Abstract

We present He isotope ( $^3\text{He}/^4\text{He}$ ) data from a fumarole and near-ground gases measured *in-situ* at the Sulfur Banks solfataras field at the summit of Kilauea Volcano, Hawaii. We used a field-deployable mass-spectrometer-based system: the Helium Isotope Monitor (HIM) previously described in McMurtry et al. (2019a, b). The *in-situ* instrument was deployed using solar power for the first time and results were ground-truthed against data determined using conventional gas analytical and noble gas mass spectrometry techniques. The HIM instrumentation, associated Vent Gas Purification System (VGPS), and related sampling equipment and strategy are described. Cloudy and rainy weather conditions hampered the deployment, which was reorganized to reduce power loads and resulted in less sampling than planned. Nevertheless, we obtained daily sampling of the volcanic vent gas. Results from the Old Well fumarole indicate a  $\sim 2 R_A$  increase in  $^3\text{He}/^4\text{He}$  on the day of the December 20th, 2020 eruption of nearby Halema'uma'u Crater, reaching  $17.0 R_A$  using the *in-situ* instrument and  $16.0 \pm 0.67 R_A$  using conventional techniques. This finding suggests that a new  $^3\text{He}$ -enriched magma source is driving the current, ongoing eruption phase of Kilauea and, if so, confirms that the deep summit caldera fault system that hosts the Sulfur Banks field is connected to the Halema'uma'u Crater magmatic system. Overall, these findings illustrate how time-series helium isotope data, which are well established by ongoing discrete monitoring at low temporal resolution, can help forecast forthcoming eruptive events that may not be foreseen by other volcanic monitoring methods.

**Keywords**  $^3\text{He}/^4\text{He}$ , Kilauea, Gas chemistry, Gas monitoring, Sulfur banks, Halema'uma'u Crater

## Introduction

Several shallow magmatic emplacements and volcanic eruptions have been documented to show precursory and synchronous changes in  $^3\text{He}/^4\text{He}$  in both gases and fluids (Sano and Wakita 1988; Sano et al. 1984, 1988, 1995, 2015; Sakamoto et al. 1992; Sorey et al. 1993; Padrón et

al. 2013; Paonita et al. 2016). Typically, these  $^3\text{He}/^4\text{He}$  variations result from injection of mantle-derived magmas that have undergone limited mixing with radiogenic crustal components into a shallow magma chamber. Depending on the magmatic system of the volcano, precursory intervals may vary from essentially synchronous (Sano et al. 1988, 1995) to a few days (Padrón et al. 2013), and up to several months or even years (Sano et al. 2015; Paonita et al. 2016). The driving mechanisms controlling the intensity and duration of precursory intervals are poorly understood (Padrón et al. 2013; Sano et al. 2015; Paonita et al. 2016).

\*Correspondence:

Gary M. McMurtry  
mcmurtry@hawaii.edu

<sup>1</sup>School of Ocean and Earth Science and Technology, Dept. of Oceanography, University of Hawaii, Manoa, Honolulu, HI 96822, USA

<sup>2</sup>School of Ocean and Earth Science and Technology, Dept. of Earth Sciences, University of Hawaii, Manoa, Honolulu, HI 96822, USA



© The Author(s) 2023. **Open Access** This article is licensed under a Creative Commons Attribution 4.0 International License, which permits use, sharing, adaptation, distribution and reproduction in any medium or format, as long as you give appropriate credit to the original author(s) and the source, provide a link to the Creative Commons licence, and indicate if changes were made. The images or other third party material in this article are included in the article's Creative Commons licence, unless indicated otherwise in a credit line to the material. If material is not included in the article's Creative Commons licence and your intended use is not permitted by statutory regulation or exceeds the permitted use, you will need to obtain permission directly from the copyright holder. To view a copy of this licence, visit <http://creativecommons.org/licenses/by/4.0/>. The Creative Commons Public Domain Dedication waiver (<http://creativecommons.org/publicdomain/zero/1.0/>) applies to the data made available in this article, unless otherwise stated in a credit line to the data.

Semi-continuous monitoring of volcanic gases and fluids may enable prediction of forthcoming eruptive events (National Academies of Sciences, Engineering, and Medicine 2017). Such monitoring is important because volcanic eruptions can be devastating to surrounding areas and populations, and are often accompanied by equally, if not more, destructive earthquakes, landslides and tsunamis (e.g., Winchester 2004; Lespez et al. 2021). Previous work primarily employed conventional sampling of gases and fluids, storage in He-leak-tight containers (i.e., glass flasks and/or copper tubes), and return to the laboratory for gas purification and analysis (e.g., Aiuppa et al. 2017). These studies are classic examples of hindcasting, as they do not allow direct monitoring of volcanic activity on a regular, (e.g., day-to-day) basis. In order to forecast eruptions, what is needed is *in-situ* analysis and monitoring by field-deployable instruments, with rapid, near real-time analysis, data storage and telemetry of the results (e.g., Wilkes et al. 2023).

Every volcano or major fault system may be affected to a certain extent by upper mantle dynamics, e.g., magma injections, gas or stress builds, on differing time scales. *In-situ* instrumentation allows eruption and earthquake forecasting scenarios to be investigated at much higher sampling frequency than before, and potentially provides continuous (e.g. near-real-time) data that could be

useful in hazards monitoring. Here we present and discuss the methodology and results of a nearly two week test deployment of the Helium Isotope Monitor (HIM) prototype *in-situ* station within the Sulfur Banks solfataria field on the summit of Kilauea Volcano, Hawaii.

## Background

### Deployment rationale

After successfully field testing the HIM *in-situ* for four months at Mammoth Mountain (CA, USA) (Hurwitz et al. 2018), where it resided in a weather-proof shelter and operated using AC grid power, we began planning for the monitoring of an active volcano where neither shelter nor grid AC power would be available. Kilauea volcano on Hawaii Island was selected due to both logistic ease and since large helium isotope anomalies are known to occur in this region (Hilton et al. 1997). The expected magnitude of the helium signal would also provide a high signal-to-noise ratio, which is critical for calibrating the instrument. The overall high frequency of eruptive activity and generally benign weather conditions also made Kilauea an ideal locality for test deployments, which were focused at the Sulfur Banks solfataria field (Fig. 1). Sulfur Banks is a well-studied volcanic system (e.g., McMurtry et al. 2019c), with several previous publications reporting its gas and isotopic chemistry (Craig and Lupton 1976;

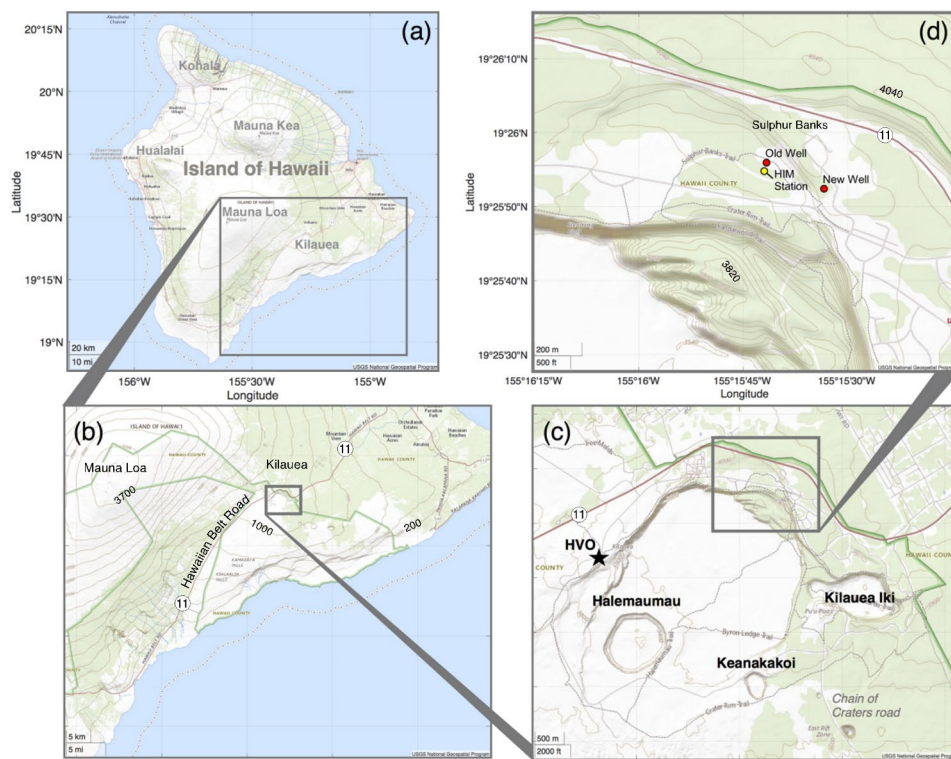


**Fig. 1** (a) Location of Kilauea Volcano on Island of Hawaii; (b) location of Kilauea summit caldera; (c) summit caldera with major features labeled, HVO = former site of Hawaiian Volcanoes Observatory; (d) Sulfur Banks solfataria field, showing locations of the Old Well (a.k.a. Jaggar Vault), New Well and Helium Isotope Monitor (HIM) Station sites. Green areas on maps are vegetated; white areas denote bare ground

Torgersen and Jenkins 1982; Friedman and Reimer 1987; Hilton et al. 1997). The challenge in our case study was to operate the prototype's relatively high-powered system on batteries charged, in this case, with solar photovoltaic (PV) panels. Choice of the time of year in Hawaii can also be important because of increasing cloudy and rainy periods between November and April. In the Sulfur Banks solfatara field, the target fumarole for our monitoring effort was the Old Well site, also known as Jaggar Vault (Allen 1922) (Fig. 1), where CO<sub>2</sub>-rich gas (~98 vol%) emanates at a maximum vent temperature of ~95 °C and has low SO<sub>2</sub> levels (~1%). The fumarole is marked by high <sup>3</sup>He/<sup>4</sup>He values that increased from 13.7 R<sub>A</sub> in April, 2018 to nearly 16 R<sub>A</sub> after the May, 2018 eruption (Peek et al. 2019, 2020).

### Description of the solar-powered HIM station

Photographs of the solar-powered station apparatus used to power the HIM *in-situ* instrument are presented in Fig. 2. The dimensions of the apparatus are 1.9 m (length) by 1.1 m (width) by 1.5 m (height). It is constructed of custom-made acid-resistant fiberglass strut and a fiberglass grate base, using stainless steel fasteners. The solar panels provide weather protection from the top and one, south facing long side, in addition to providing solar PV power. The major components of the *in-situ* instrument are as follows.

- (1) Helium Isotope Monitor (HIM) (Fig. 3).
- (2) Vent Gas Purification System (VGPS) (Fig. 4).
- (3) An internal panel that provides mounting for two solar panel controllers, a junction box tying three of the 55 W panels together, and a 500 W DC-AC inverter.
- (4) Four deep-cycle, rechargeable Pb-acid gel cell batteries, connected in parallel at 12 V (300 amp-hrs. total capacity).
- (5) A compressed dry nitrogen gas cylinder.
- (6) Glass water condensation trap.
- (7) Water vapor condensation cooler based upon a modified portable thermoelectric refrigeration unit (Koolatron™).

The HIM and VGPS units have been described previously in McMurtry et al. (2019a, b). The core of the Helium Isotope Monitor (HIM) (Fig. 3) is a NEG-Ion vacuum system with a quartz glass membrane, two mass spectrometers, and a full-range pressure gauge. The NEG pump allows accumulation of noble gases and the noble ion pump is used to clean the high vacuum between samples. The primary mass spectrometer is a frequency-modified, high-resolution quadrupole with a mass range from 1 to 6 amu (MKS Microvision2), and the secondary mass spectrometer is an asynchronous ion trap (ART) with a mass range

from 1 to 150 amu (components 2 and 6 in Fig. 3, respectively). Both Mass Spectrometer (MS) units are made by MKS Instruments, Inc. The MKS quadrupole is high resolution, but not high enough to resolve the extremely tight isobaric interference of HD with <sup>3</sup>He. We therefore employ an Adjusted Ionization Mass Spectrometry (AIMS) technique (TIMS technique of Davies et al. 2014) and use the programmable capability of the MKS Microvision2 to adjust the ionization of the selected species 'on the fly'. We obtain <sup>3</sup>He partial pressure (PP) from the net of the total pressure response at m/z=3.0 and the PP response for HD alone, after lowering the ionization potential from the customary 70 eV to under 30 eV. The <sup>4</sup>He response is measured at the m/z=4.0 address and the H<sub>2</sub> response at the m/z=2.0 address on the same sample at the same time, with no 'tailing' effects despite the extremely large abundance differences. These measurements are done sequentially within microseconds and the whole sequence is repeated until sufficient mass response is attained. The quadrupole multiplier detector has a 10<sup>7</sup> gain, which can be adjusted to accommodate anticipated differences in response based upon species abundance. The ion trap MS can also obtain <sup>4</sup>He and H<sub>2</sub> response data and is used to monitor overall high vacuum quality. These data are stored in flash memory on a 'master' Rabbit™ microprocessor and embedded PC, and can be manipulated to display calculated data in real time and telemetered to remote sites.

The Vent Gas Purification System (VGPS) (Fig. 4) was developed primarily to reduce water vapor loads to the HIM sample chamber. Water is a very small molecule that can diffuse through quartz glass and potentially saturate the high vacuum NEG pump. Its presence as dominantly meteoric water also dilutes the measured abundance of other gases and is of little importance to most volcanic studies unless magmatic water is of interest (e.g., Goff and McMurtry 2000). The water is removed by adsorption onto chemical getters, in this case two cartridges filled with Drierite™ indicating calcium sulfate (anhydrite) and one cartridge filled with indicating molecular sieve. The pumped gas flow is by way of a four-diaphragm KNF pump equipped with custom Teflon™ diaphragms and Valcor™ Teflon™ solenoid valves to direct flow. Direct sample drying is followed by sample recirculation to maximize exposure to the chemical getters. Besides water, any sulfur gases present will be scrubbed by these getters, especially in the presence of water, so their detection should be made prior to VGPS treatment. A second, 'slave' Rabbit™ microprocessor is programmed to direct the sample purification sequence via a series of valve relays on the control electronics board. The sampling sequence is started by evacuation of the sample chamber to 2–4 Torr.



**Fig. 2** Photographs of the December 2020 deployment. **(a)** Solar-power equipped HIM Station with additional rain protection, looking east. **(b)** Internal layout (see text for detailed description of components). **(c)** Wide view of Sulfur Bank, looking NW. The Old Well fumarole is circled in red and the HIM solar station, which is located approximately 9 m S-SE on bare ground, is circled in yellow

A feature of the VGPS is a two-way intake selection, using a Valcor two-way gradient valve that allows switching between volcanic vent and ambient samples. The HIM auto run program defaulted to ambient intake

every time the instrument was re-activated, which had to be done every day to conserve battery power. Several attempts to manually override this default selection to vent or fumarole intake were unsuccessful, so we

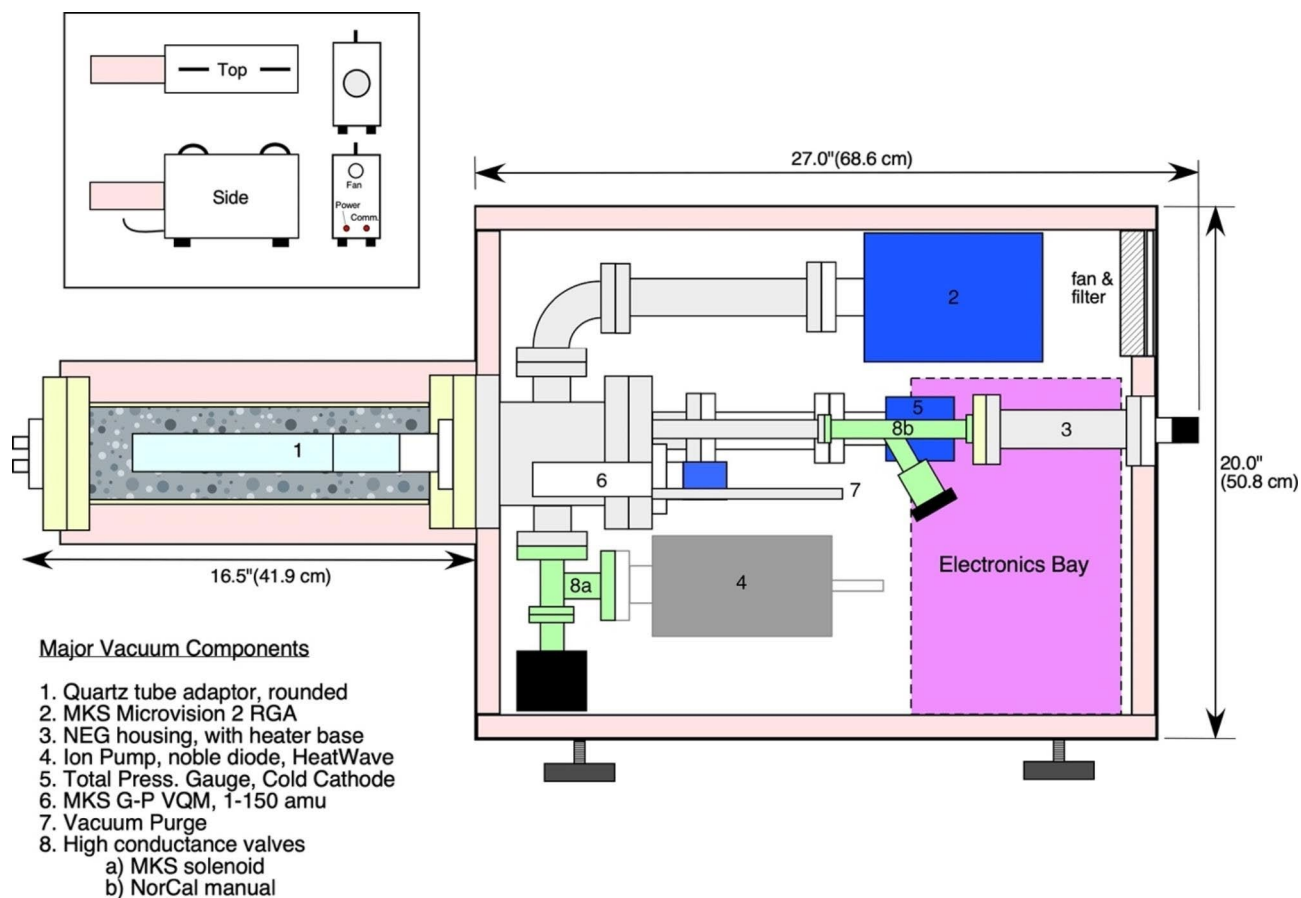


**Fig. 3** Schematic diagram of the portable field Helium Isotope Monitor (HIM), showing major vacuum components. Electronics and wiring are not shown for clarity. Pink areas indicate thermal insulation. A detailed description of the working procedure for this instrument can be found in the text and in McMurtry et al. (2019a, b)

collected more ambient or near-ground gas samples than originally planned.

The large glass REC™ panel provided 375 W of charging power to three of the four batteries. It was chosen for its high-efficiency (21%) energy production and rugged construction, allowing for no additional support, which kept the overall station weight low. The three rugged plastic Ganz™ panels provided a total of 165 W of charging power to one battery that was dedicated to the thermoelectric refrigeration unit. For this deployment, the data were recorded to internal flash memory cards, although remote communication by cell phone is possible from our sampling site, as was previously employed at Mammoth Mountain (Hurwitz et al. 2018).

#### Field sampling protocol for Kilauea

For the Kilauea Sulfur Banks, because the Old Well (a.k.a. Jaggar Vault) fumarole is located close to the wooden pedestrian walkway, the National Parks Service sampling permit requires that the HIM station be located at some prudent distance away so as to not interfere with the visitor experience and prevent any potential tampering,

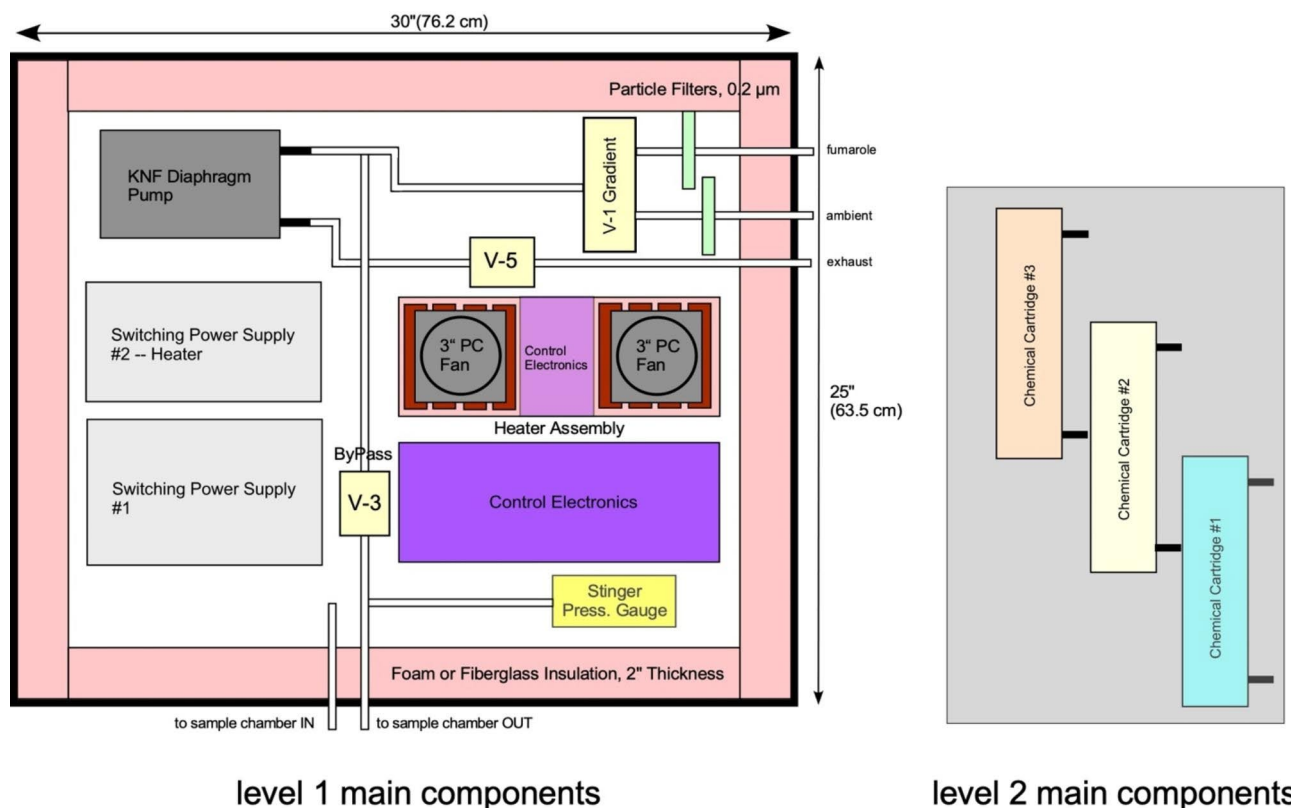
with no unauthorized foot traffic allowed off the walkways. The field layout is presented in Fig. 5. To our pleasant surprise, the extended tubing to the station acted like a water vapor condensation line, so the Koolatron™ cooler was therefore not needed and was removed after a few days, which saved on power consumption. Ground-truthing gas samples were collected throughout the field deployment period at the two areas indicated in Fig. 5. Sampling consisted of filling evacuated Giggenbach glass flasks, immediately followed by gas pumped through copper tube samplers, which were crimped for later analysis of helium and its isotopes plus other noble gases.

#### Ground-truth and conventional supplementary methods

##### *Analytical techniques—Barry Lab, Woods Hole Oceanographic Institution*

Helium and neon isotope analyses were conducted in the Barry Lab at Woods Hole Oceanographic Institution (WHOI) on a Nu Instruments multi-collector Noblesse HR mass spectrometer (Barry et al. 2022). The Noblesse has the capability to determine the isotope ratios of all 26 stable noble gases and a unique zoom optics system

## Vent Gas Purification System (VGPS)



level 1 main components

level 2 main components

**Fig. 4** Schematic diagram of the Vent Gas Purification System (VGPS). All components fit within a portable Pelican™ case. Three removable chemical cartridges clamp onto the top layer (level 2) with two DC power supplies and a customized Teflon™ KNF diaphragm roughing pump located below (level 1). Internal Valcor™ Teflon™ solenoid valves direct gas flow; valves 1 (gradient), 3 (by-pass) and 5 (exhaust) are indicated. Pressure is measured with an InstruTec™ Stinger convection gauge. A custom command electronics board relays valve openings, temperatures, pressures and roughing pump on/off via a Rabbit™ microprocessor. A small heater assembly is used for extremely cold environments. The VGPS is also insulated with closed-cell foam. A detailed description of the working procedure for this instrument can be found in the text and in McMurtry et al. (2019a, b)

that allows for instantaneous switching between different isotope sets. The zoom optics permit the detectors to be fixed, greatly enhancing reliability. The sensitivity and resolving power are also adjusted without the complexity of a movable source slit. The instrument is interfaced to a noble gas processing and purification inlet system that is fully automated.

### Gas sample noble gas purification

Cu tube samples were connected to the extraction line using an O-ring connection and  $\sim 5 \text{ cm}^3$  of gas was expanded into the cleanup line. The pressure was measured using a capacitance manometer and then a small aliquot of gas was expanded into the cleanup portion of the line. Reactive gases were chemically removed by exposing gases to a titanium sponge held at  $650 \text{ }^\circ\text{C}$ . A full description of the WHOI noble gas cleanup procedure is described in Barry et al. (2022).

### Analytical techniques—Fischer Lab, University of New Mexico

The samples were collected in evacuated Giggenbach flasks that did not contain a caustic solution and were analyzed by a combination of gas chromatography (GC) and quadrupole mass spectrometry (QMS) following the procedure described in Lee et al. (2017). The gas chromatograph separates  $\text{CO}_2$ ,  $\text{H}_2$ ,  $\text{N}_2$ ,  $\text{Ar} + \text{O}_2$ ,  $\text{CH}_4$  and  $\text{CO}$ . The quadrupole is used in dynamic mode to analyze He, Ar,  $\text{N}_2$  and  $\text{O}_2$ . In the sample preparation line and prior to admission to the GC and QMS, samples are exposed to a dry-ice ethanol mix to remove water vapor. The gas is admitted to the GC via a combination of 6 and 10 port valves. The gas enters the QMS via a variable leak valve that reduces the pressure of the sample from a pressure of several 10's of Torr to the  $10^{-7}$  Torr level in the QMS. Calibration gas mixtures are used for both instruments. For the QMS, the calibration gas mix contains 1000 ppm He, 1% Ar, 21%  $\text{O}_2$  and 78%  $\text{N}_2$  and the signal from Ar in the calibration gas mixture is adjusted using the leak

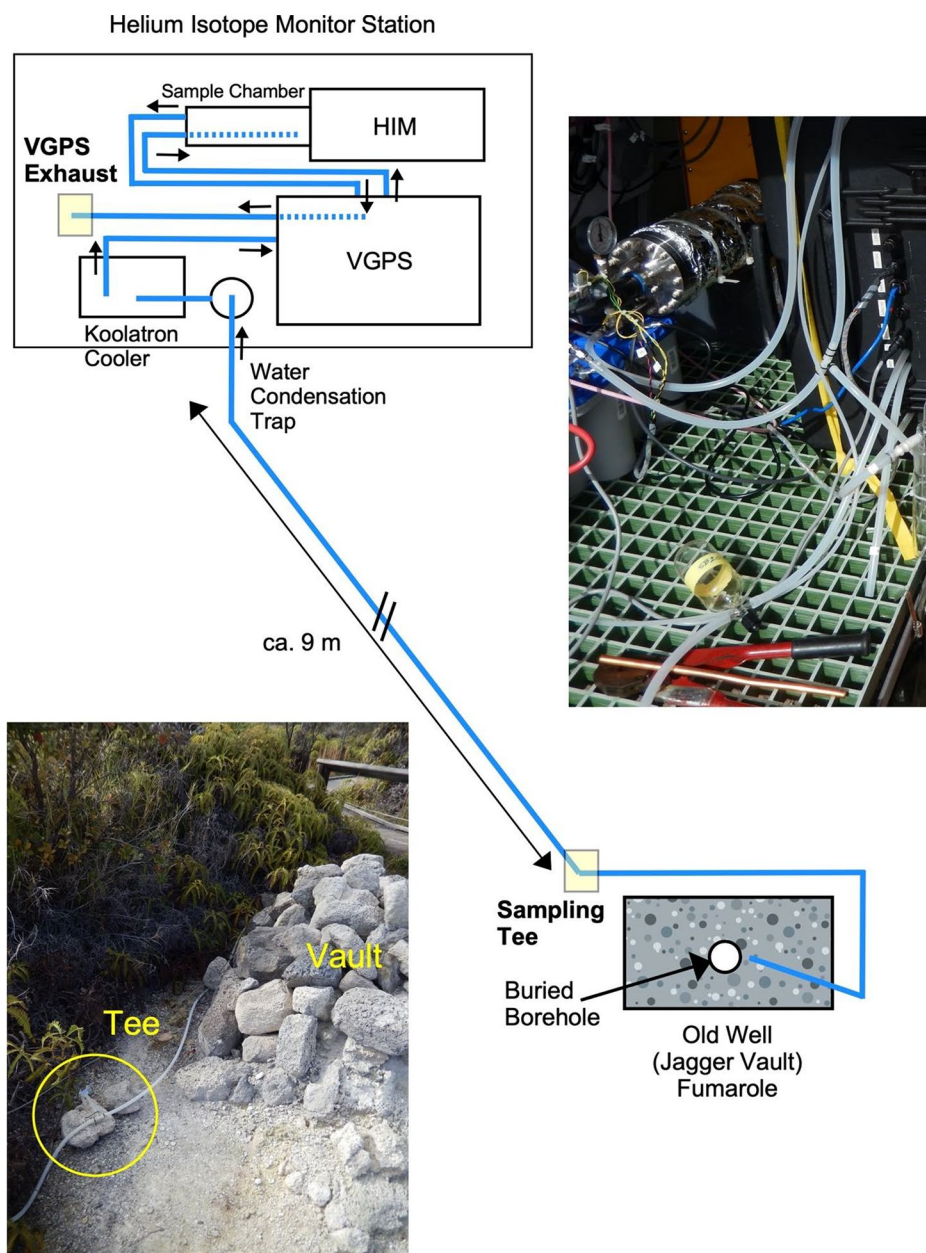


**Fig. 5** Schematic diagram of the HIM station sampling layout at the Old Well fumarole, Sulfur Banks solfatara field, Kilauea. See Fig. 2c for large area view. Small arrows in the HIM station box indicate direction of pumped gas flow through the thick-walled, flexible silicone tubing, denoted by blue lines. The two main areas designated for ground-truth sampling are at the VGPS pump exhaust and the sampling Tee. TOP INSERT: photo of manual sampling at VGPS exhaust hose. An evacuated Giggenbach sampler is in place. A copper tube and manual cold welder (Team product) is nearby. BOTTOM INSERT: photo of the sampling Tee established near the Old Well fumarole. The borehole is the top of the original well, now buried under rocks. Directional flow gas samples were obtained by changing the position of the hose clamp from the short 90° tube to the longer tubing connected to the HIM station. Those samples were obtained by manual hand pumping, following standard field protocols (e.g., Hunt et al., 2015)

valve to that expected for the samples. For example, the Ar signal during calibration was adjusted to  $2.5 \times 10^{-9}$  A and the Ar signal from sample SB020-1,  $2.21 \times 10^{-9}$  A or within about 10% of the calibration value. For some samples the Ar signal was significantly lower than that of the calibration signal. These Samples SB02-2, SB020-6,

SB020-8 and SB020-12 were re-analyzed after a new QM calibration at lower Ar signal to match the sample signal. We report herein the relative molar abundances of CO<sub>2</sub>, H<sub>2</sub>, Ar, O<sub>2</sub>, N<sub>2</sub>, CH<sub>4</sub> and CO of the samples collected. Helium data were collected but are not reported because

of an unresolved calibration issue with the quadrupole MS.

## Results

### *He isotopes with the HIM in-situ instrument — a timeseries analysis*

HIM analyses began on 8 December 2020 (Table 1) with conventional ground-truthing sampling on 10 December 2020 (Table 2). The conventional He isotope results for the near-ground and fumarole samples collected

on December 10–15, 2020 range from 0.8 to 1.1  $R_A$  (Table 2; Fig. 6). These air-like values make more sense for the instrument pump exhaust samples (samples SB20-1,3,5,7) than for those taken subsequently at the Tee near to the fumarole by hand pumping (samples SB20-2,4,6,8). Either the sample tubing to the fumarole was not adequately flushed *in-situ* or the sample sealed within the copper tube was contaminated with air, either upon crimping (the cold weld on the copper tube did not hold), storage before analysis or during the sample extraction

**Table 1** “Edward” Prototype Helium Isotope Monitor (HIM) Data, Sulfur Banks, Kilauea, December 2020 Deployment

Conventional Sample ID	Collection Date	$^3\text{He}$ (Torr)	$^4\text{He}$ (Torr)	$^3\text{He}/^4\text{He}$	R/Ra *	Rc/Ra **	Rc/Ra ***	Rc/Ra #	Comments
	12/8/20	1.86E-11	9.10E-07	2.04E-05	3.3	n.d.	n.d.	---	Near-ground gas
	12/9/20	2.41E-11	1.02E-06	2.37E-05	3.8	n.d.	n.d.	---	Near-ground gas
<b>SB 20-1, SB 20-2</b>	12/10/20	1.68E-11	8.25E-07	2.03E-05	3.3	n.d.	n.d.	0.8, 1.3	Near-ground gas
	12/11/20	2.21E-11	9.95E-07	2.23E-05	3.6	n.d.	n.d.	---	Near-ground gas
<b>SB 20-3, SB 20-4</b>	12/12/20	1.75E-11	8.16E-07	2.14E-05	3.5	n.d.	n.d.	1.1, 0.7	Near-ground gas
<b>SB20-5, SB20-6</b>	12/13/20	---	---	---	---	---	---	0.3, 1.4	No monitor sample
	12/14/20	1.96E-11	9.72E-07	2.02E-05	3.3	n.d.	n.d.	---	Near-ground gas
<b>SB20-7, SB20-8</b>	12/15/20	1.47E-11	8.03E-07	1.83E-05	3.0	n.d.	n.d.	n.d., 1.4	Near-ground gas
	12/16/20	1.01E-11	8.09E-07	1.24E-05	2.0	2.0	2.5	---	intakes joined to fumarole
<b>SB20-9, SB20-10</b>	12/17/20	3.91E-11	1.43E-06	2.73E-05	4.4	12.8	15.7	14.3, 14.8	fumarole
	12/18/20	3.21E-11	1.20E-06	2.68E-05	4.3	12.4†	15.2†	---	fumarole
<b>SB20-11, SB20-12</b>	12/19/20	3.39E-11	1.09E-06	3.12E-05	5.0	12.2	15.0	2.0, 1.2	fumarole
<b>SB20-13, SB20-14</b>	12/20/20	3.68E-11	1.06E-06	3.47E-05	5.6	13.8†	17.0†	16.0, 15.0	fumarole
<b>Lab air series</b>	1/20/21	9.24E-12	9.29E-07	9.95E-06	1.6	---	---	---	lab air, good signal
	1/22/21	2.91E-12	9.89E-07	2.94E-06	0.5	---	---	---	lab air; low signal
	1/25/21	5.87E-12	9.91E-07	5.92E-06	1	---	---	---	lab air, OK signal
	2/1/21	5.81E-12	7.66E-07	7.58E-06	1.2	---	---	---	lab air, OK signal
	2/2/21	4.91E-12	7.52E-07	6.53E-06	1.1	---	---	---	lab air, OK signal
	2/9/21	3.31E-12	7.80E-07	4.24E-06	0.7	---	---	---	lab air, low signal
Lab air average	1–2/21	5.34E-12	8.68E-07	6.16E-06	1.0	---	---	---	Std. dev. = 0.39

\*  $R/Ra = [^3\text{He}/^4\text{He}]_{\text{sample}} / [^3\text{He}/^4\text{He}]_{\text{air}}$ , where  $[^3\text{He}/^4\text{He}]_{\text{air}}$  is the average of the lab air series in Table 1 obtained in Jan and Feb 2021

\*\* Corrected for air contamination using the mixing equation in McMurtry et al. (2019b) and the Ar values reported in Table 3. An average error of 7.9% (n=7) was calculated from the difference between the expected  $\text{CO}_2$  concentration of 98% in pure vent gas (Naughton et al. 1973; Peek et al. 2020) from those calculated using the fumarole gas fraction in Table 3. SB ambient samples were not corrected

\*\*\* Corrected minimum values from highest  $^3\text{He}/^4\text{He}$  response of three runs of the helium standard of Japan (HESJ) standard from July 2021, where the accepted value for the standard is 20.6 R/Ra (Masuda et al. 2002). The highest value of 15.9 Ra was 23% lower; the average minimum response of  $14.8 \pm 1.0$  Ra was 28% lower than the previous instrument calibration

# Conventional analysis of Cu-tube samples (see Table 2). First value per day was taken at VGPS pump exhaust; second value was taken at Tee near fumarole with hand pump (see Fig. 5)

† Using Ar concentration value from previous day

**Table 2** Conventional Helium Isotope Data, Sulfur Banks, Kilauea, December 2020 Deployment†

Conventional Sample ID	Collection Date	Location Type	R/R <sub>a</sub>	R <sub>c</sub> /R <sub>a</sub>	<sup>4</sup> He/ <sup>20</sup> Ne	X-value*	<sup>4</sup> He (cm <sup>3</sup> STP/cm <sup>3</sup> )	<sup>20</sup> Ne (cm <sup>3</sup> STP/cm <sup>3</sup> )	<sup>40</sup> Ar (%)**	Comments
SB 20-1	12/10/20	VGPS Exhaust	1.0	n.d.	0.3	0.9	4.06E-06	1.35E-05	0.6936	OK
SB 20-2	12/10/20	Tee near fumarole	1.0	n.d.	0.3	0.8	4.20E-06	1.56E-05	0.8015	Sample Lost***
SB 20-3	12/12/20	VGPS Exhaust	1.0	n.d.	0.3	0.9	4.00E-06	1.37E-05	0.7038	OK
SB 20-4	12/12/20	Tee near fumarole	1.0	n.d.	0.3	0.9	3.68E-06	1.32E-05	0.6782	Sample Lost?
SB20-5	12/13/20	VGPS Exhaust	1.0	n.d.	0.3	1.0	4.99E-06	1.62E-05	0.8323	OK
SB20-6	12/13/20	Tee near fumarole	0.8	n.d.	0.2	0.7	3.49E-06	1.55E-05	0.7963	Sample Lost***
SB20-7	12/15/20	VGPS Exhaust	1.1	n.d.	0.3	0.9	4.50E-06	1.56E-05	0.8015	OK
SB20-8	12/15/20	Tee near fumarole	0.9	n.d.	0.3	0.9	4.11E-06	1.52E-05	0.7809	Sample Lost***
SB20-9	12/17/20	VGPS Exhaust	10.4	14.3 ± 0.34	1.1	3.4	6.44E-06	5.88E-06	0.3021	OK
SB20-10	12/17/20	Tee near fumarole	14.6	14.8 ± 0.52	18.9	59.5	4.78E-06	2.52E-07	0.0129	OK
SB20-11	12/19/20	VGPS Exhaust	0.9	n.d.	0.3	0.9	4.83E-06	1.63E-05	0.8374	Sample Lost***
SB20-12	12/19/20	Tee near fumarole	1.0	n.d.	0.3	0.9	4.76E-06	1.62E-05	0.8323	Sample Lost***
SB20-13	12/20/20	VGPS Exhaust	11.2	16.0 ± 0.67	1.0	3.1	4.94E-06	4.95E-06	0.2543	OK
SB20-14	12/20/20	Tee near fumarole	14.8	15.0 ± 0.53	31.5	98.9	4.48E-06	1.42E-07	0.0073	OK
SB20-15	12/20/20	Tee near fumarole	15.0	15.1 ± 0.20	35.6	124	6.06E-06	1.70E-07	0.0088	OK

† All samples were collected in crimped copper tubes after pumping gas through them, either automatically or by hand. Samples SB20-1 through SB20-14 were analyzed in the Barry Lab at WHOI. Replicate sample SB20-15 was analyzed by A. Hunt, USGS Denver Isotope Lab; this sample was 99.0% CO<sub>2</sub>. Detailed analysis procedures can be found in Hunt (2015)

\* X value is calculated as the <sup>4</sup>He/<sup>20</sup>Ne of the sample over the <sup>4</sup>He/<sup>20</sup>Ne of air

\*\* Calculated using <sup>20</sup>Ne/<sup>40</sup>Ar and assuming <sup>20</sup>Ne and <sup>40</sup>Ar concentrations of 0.00001818 and 0.00934 mol/mol for pure dry air, respectively

\*\*\* Air compositions are due to sample gases being overwhelmed by air contamination. Air corrections (R<sub>c</sub>/R<sub>a</sub>) are not included for samples with <sup>4</sup>He/<sup>20</sup>Ne values below 1.0, because the correction breaks down (P. Barry, pers. comm., 2022)

process. In our field protocol (see Sect. 2.3), the copper tube samples were taken immediately after the Giggenbach evacuated samples, which unless noted otherwise, were sampling highly CO<sub>2</sub>-enriched gas (Table 3; Fig. 7). Therefore, we suspect that these samples were contaminated prior to isotopic analysis. They are denoted with question marks in Fig. 6 and have implications for the companion samples taken at the instrument pump exhaust (see Discussion Sect. 4.3).

After measuring the dilute near-ground gas, we used the HIM to analyze gases from the Old Well fumarolic vent on December 16–20, 2020 (Table 1). Here gas was pumped at a rate of 4 L/min from the vent through the condensation traps, VGPS and HIM sample chamber, using a KNF™ diaphragm pump equipped with acid-resistant Teflon diaphragms and anodized Al blocks. Five minutes of pumping was sufficient to evacuate over four volumes of the total sampling system. In addition, we took conventional gas samples (in evacuated Giggenbach gas bottles and crimped copper tubes for helium) from the pumped exhaust after three minutes of pumping and

at a sampling Tee placed in the tubing closer to the fumarole immediately after VGPS pumping had ceased (Fig. 5; Tables 1 and 2).

The measured He isotope value dropped to a low of 2.0 R<sub>c</sub>/R<sub>a</sub> on the 16th of December when the two intake lines, ambient and fumarole, to the VGPS were merged (Table 2; Fig. 6). The probable source for this abrupt drop in the helium isotope ratio is air that diffused or leaked into the long tube running to the station. The other (less likely) possibility could be the loss of <sup>3</sup>He-rich helium by diffusion during prolonged storage within the thick-walled silicone tubing used.

The Old Well vent was more effectively sampled from December 17th to 20th. The most important observed aspect was operational. The sample line now drew pumped vent gas from the fumarole, without a change in vent gas composition (Table 1; Fig. 6). Evidence for this improved sampling and gas pumping from the fumarole included the presence of water vapor condensate in the condensation trap, observation of warm gas in the tubing, and a distinct H<sub>2</sub>S-generated odor to the

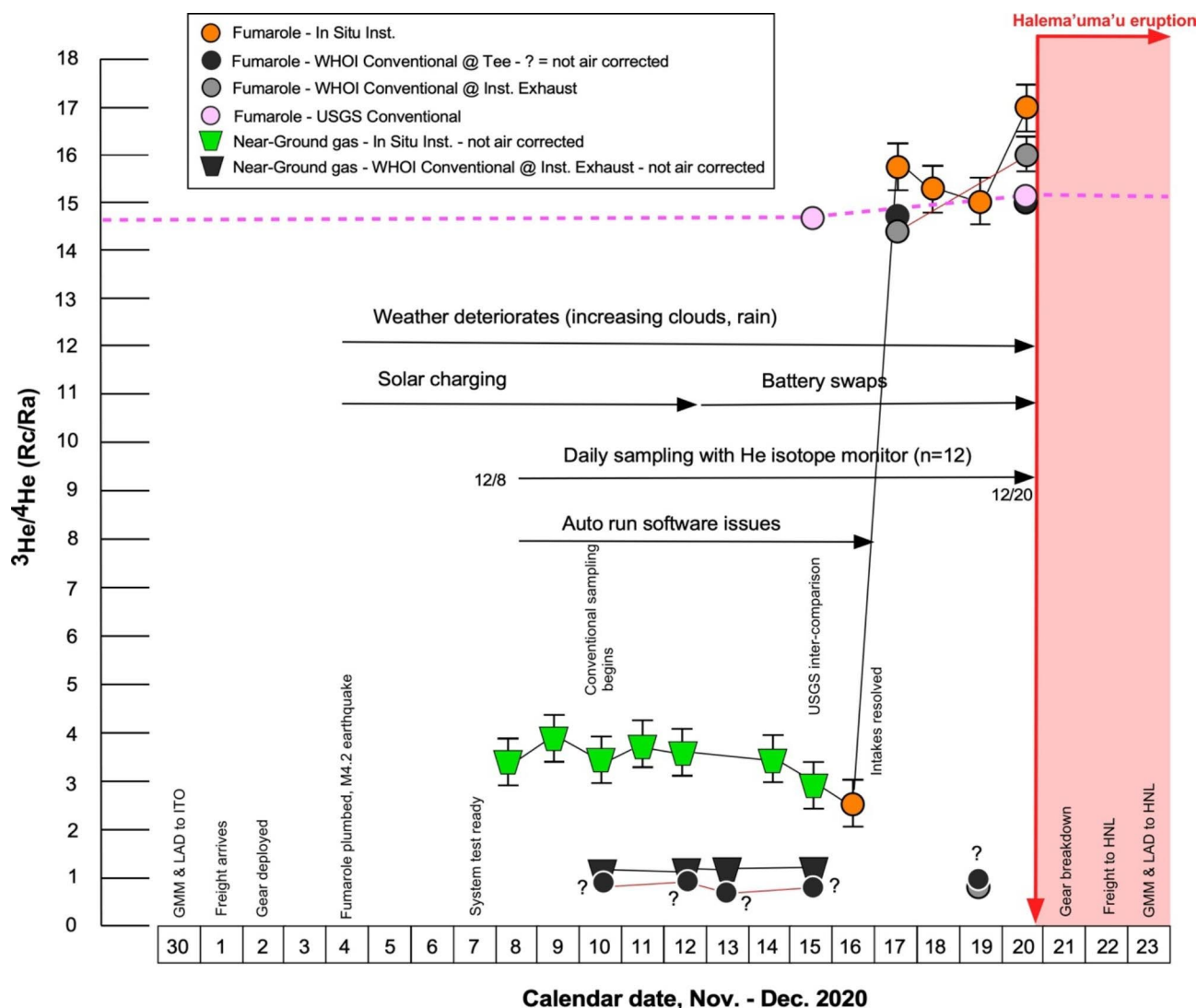


**Fig. 6** Timeseries of  $^3\text{He}/^4\text{He}$  as  $R/R_A$  and  $R_C/R_A$  ratios from the December 2020 deployment, with significant events marked. Except as noted,  $R_C/R_A$  for the instrument and conventional samples are plotted versus the collection date. Sample type is depicted by the symbols (see legend). All data from Tables 1 and 2 as well as the Dec. 15th  $^3\text{He}/^4\text{He}$  fumarole data (USGS, A. Hunt, analyst) provided by T. Nadeau (pers. comm., 2021). Estimated 0.5  $R_C/R_A$  errors are assigned to the HIM data reported in Table 1; other errors are from values reported in Table 2 or are within the symbols

pump exhaust. Elevated  $\text{CO}_2$  and low Ar concentrations also support this assertion. The uncorrected helium isotope value rose to 4  $R_A$  for two days and then gradually increased to  $\sim 5.6 R_A$  on December 20th, our last day of collection. Kilauea's nearby Halema'uma'u Crater erupted at about 21:30 local time on 20 December 2020, and continued for five months. In September 2021, the eruption resumed in the crater and, with a few hiatuses, continued to March, 2023 (see: <https://www.usgs.gov/volcanoes/kilauea/volcano-updates>).

Two-component mixing corrections for air contamination yield increasing air-corrected He isotope ( $R_C/R_A$ ) values from 15 to 17 on December 17–20 (Table 1; Fig. 6). These air corrections involved using the measured Ar concentrations in companion samples (Table 3). We used

the same procedure and assumptions as in McMurtry et al. (2019b); who proposed a modification of the known He isotope air-correction method using  $^4\text{He}/^{20}\text{Ne}$  ratios (Sano and Wakita 1985), using  $^{40}\text{Ar}$  instead of  $^{20}\text{Ne}$ , and which requires knowledge of the pure volcanic vent  $^{40}\text{Ar}$  abundance. The air correction method uses a two-component mixing of pure fumarole gas and ambient air. Using argon as a conservative air signature gas, we calculate an algebraic equation using a value of 0.0024% on a dry basis for Ar from a 308 °C fumarole sample collected at the base of the Halema'uma'u Crater (Sample KV97-3; Elias 1999) in May 1997. For dry air, we used a value of 0.93%. Following McMurtry et al. (2019b), the mixing equation for an arbitrary Kilauea Sulfur Banks sample is as follows.

**Table 3** Chemical composition of Sulfur Banks gases, Kilauea

Sample ID	Date	Location Type	Sample Type	in mol %						
				CO <sub>2</sub>	calc. CO <sub>2</sub> *	H <sub>2</sub>	Ar	O <sub>2</sub>	N <sub>2</sub>	CH <sub>4</sub>
SB20-1	12/10/20	VGPS Exhaust, VGPS pumped	near-ground gas	0.0710	---	-	0.8805	20.34	78.71	-
SB20-2	12/10/20	Tee near fumarole, hand pumped line	fumarole	92.34	99.6	0.1299	0.0683**	0.25	6.99	0.0110
SB20-3	12/12/20	VGPS Exhaust	near-ground gas	0.0800	---	0.0070	0.8441	20.18	78.88	-
SB20-4	12/12/20	Tee near fumarole, bad valve on bottle	fumarole	---	---	---	---	---	---	---
SB20-5	12/13/20	VGPS Exhaust	near-ground gas	0.1081	---	-	0.8036	18.92	80.16	-
SB20-6	12/13/20	Tee near fumarole	fumarole	39.15†	85.6	-	0.5059	11.26	49.08	-
SB20-7	12/15/20	VGPS Exhaust	near-ground gas	0.0810	---	-	0.8623	19.78	79.28	-
SB20-8	12/15/20	Tee near fumarole	fumarole	92.75	95.9	-	0.0329**	0.66	6.41	0.0020
SB20-9	12/17/20	VGPS Exhaust	fumarole-inst.	24.91†	86.0	0.0150	0.6617	14.16	60.26	-
SB20-10	12/17/20	Tee near fumarole	fumarole	60.46†	88.0	-	0.2930	6.84	32.40	0.0010
SB20-11	12/19/20	VGPS Exhaust	fumarole-inst.	31.20†	86.9	-	0.5971	12.75	55.45	-
SB20-12	12/19/20	Tee near fumarole	fumarole	92.21	92.7	0.0430	0.0438**	1.03	6.56	0.0020
Dry air	-----	-----	ambient	0.0412	---	0.000003	0.934	20.95	78.08	0.0002

'-' is not detected; '---' is no data

SB20-4 had a bad valve, could not be opened

Analyzed by T Fischer, University of New Mexico. February 2021

\* Calculated with fumarole gas fraction from Ar conc., using mixing equation from McMurtry et al. (2019b)

\*\* Results from second run of these samples

† Sample bottle may have lost partial vacuum

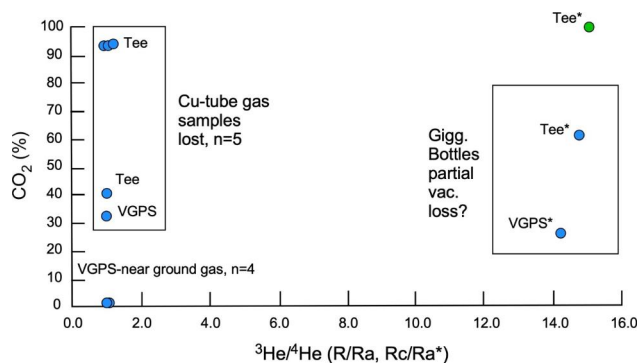


**Fig. 7** Carbon dioxide (CO<sub>2</sub>) versus <sup>3</sup>He/<sup>4</sup>He (R/R<sub>A</sub>, R<sub>C</sub>/R<sub>A</sub>) ratios for ground-truthing samples from data in Tables 2 and 3. All CO<sub>2</sub> results from companion Giggenbach bottle samples were taken sequentially prior to copper tube samples taken for helium and isotopes. The one exception (green dot) was a CO<sub>2</sub> analysis from the same copper tube sample (SB20-15, Table 2) analyzed by the USGS. The location of the sample sites is noted. Because low, air-like He isotope (R/R<sub>A</sub>) ratios for high CO<sub>2</sub> content gas is unlikely, at least five fumarole-like gas samples (see left rectangle) were contaminated, either upon line flushing, tube crimping, storage or sample extraction. Partial vacuum loss (see right rectangle) refers to samples that may have lost part of their original vacuum. Samples labeled VGPS were vigorously pumped by an electric diaphragm pump; all others were manually pumped with a piston hand pump

Ar(pure fumarole) + (1 - x) Ar(air) = Ar(measured);  
 $0.0024x + (1 - x) (0.93) = 0.60$ ;  $x = 0.356$ , where  $x$  = the fumarole gas fraction.

A further minimum correction was made for decreasing mass spectrometer sensitivity over time, using the helium standard of Japan (HESJ) isotopic standard (Table 1, footnote). These same magmatic fractions were used to correct the measured CO<sub>2</sub> concentrations up to those expected in the pure vent samples (Table 3). These calculated concentrations are nearly the same as or less than those expected, suggesting that in some cases the CO<sub>2</sub> concentrations were under-corrected.

#### <sup>4</sup>He concentration

Table 2 shows <sup>4</sup>He concentrations as cm<sup>3</sup>STP/cm<sup>3</sup> (i.e., ppm × 10<sup>6</sup>) in the conventional copper tube He splits. Additional molar concentrations of H<sub>2</sub>, Ar, O<sub>2</sub>, N<sub>2</sub>, CH<sub>4</sub> and CO in samples collected in evacuated Giggenbach glass bottles are reported in Table 3. At present, total <sup>4</sup>He concentrations from the HIM are not calibrated and reported as instrument response in partial pressure (Torr units) in Table 1. A good correlation exists between the HIM response and <sup>4</sup>He concentrations reported by the Barry Lab from corresponding copper tube samples (Fig. 8). The <sup>4</sup>He data presented in Table 2 are generally lower (3.5 to 6.4 ppm) but comparable with previous <sup>4</sup>He data obtained by using the same methodology at Sulfur

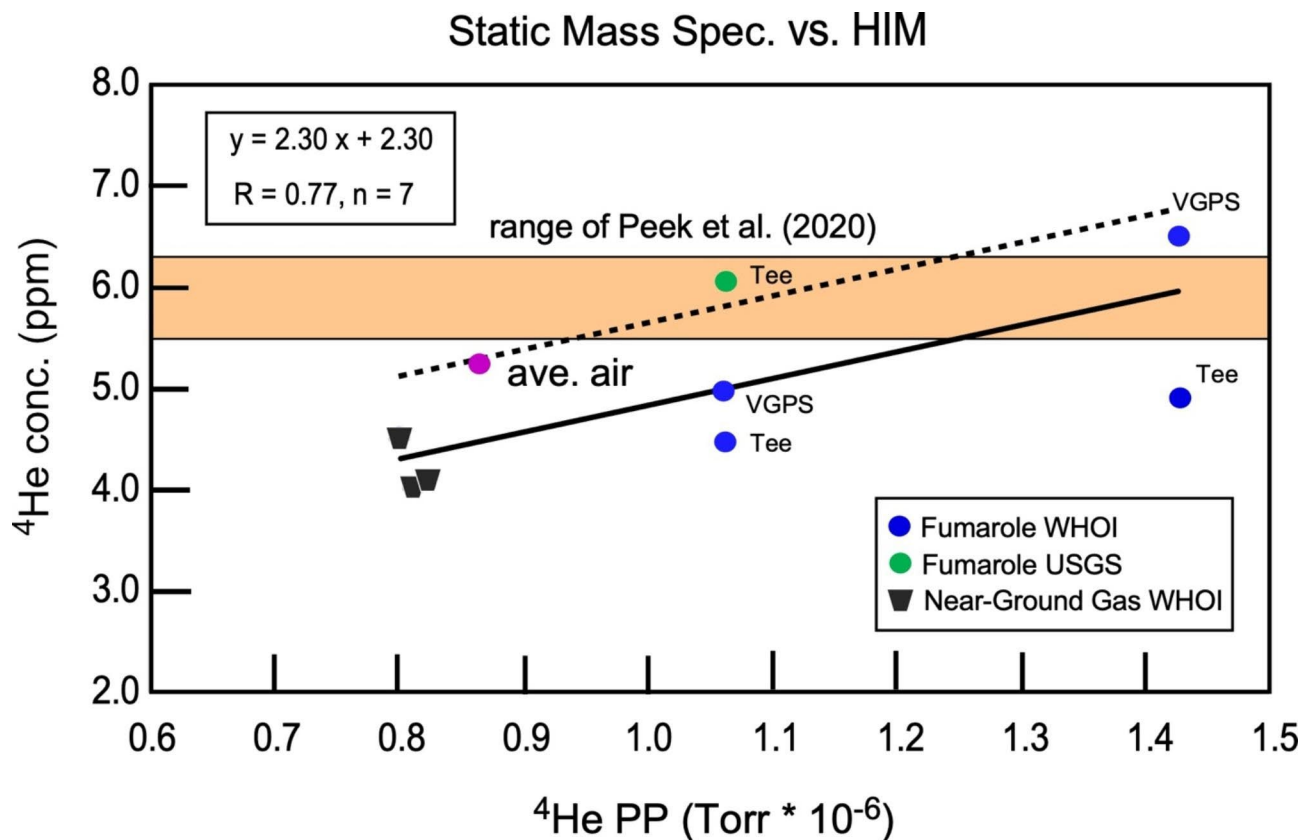


**Fig. 8** Correlation plot of  $^4\text{He}$  concentration (in ppm) reported by the Barry stable isotope lab, Woods Hole Oceanographic Institution (WHOI) (Table 2) versus the corresponding  $^4\text{He}$  instrument response as partial pressure (PP) in Torr (Table 1). Solid black line is least-squares regression fit to the WHOI fumarole and near-ground gas data. Dashed line is suggested correlation fit if there is a downward calibration offset to the WHOI  $^4\text{He}$  data, which is strongly suggested by the lower-than-air  $^4\text{He}$  values for the three near-ground gas samples (see text for explanation). Orange rectangle shows the  $^4\text{He}$  (ppm) range of Peek et al. (2020)

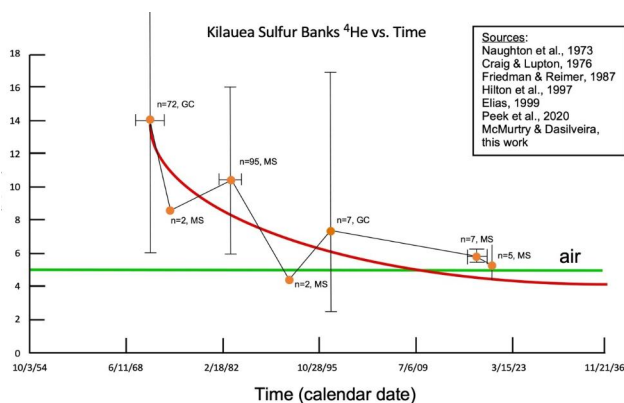


**Fig. 9** Timeseries of  $^4\text{He}$  concentration (in ppm) in vent gas collected at the Old Well and New Well sites from early 1970 until late 2020. Data sources are noted. Except for the standard deviation error bars of Naughton et al. (1973), we report the mean and range of concentrations for the monitoring period, the latter denoted as horizontal bars. Also reported are the number of samples and the method used to determine the helium values (GC: gas chromatography, MS: mass spectrometry). The red solid curve is a suggested long-term trend to these data. The green solid line indicates the average air concentration

Banks (Peek et al. 2020) (Fig. 8). We are therefore, confident about the He concentrations measured by the HIM at the Old Well vent.

Previous work on helium at Sulfur Banks indicates that the gas varies widely in concentration over time (Fig. 9). Beginning in 1964, monitored  $^4\text{He}$  concentrations ranged from 4 to 75 ppm on a dry-gas basis (with spikes to ~40 ppm from 1970 to 1972), assuming  $92 \pm 2\%$  measured  $\text{H}_2\text{O}$  and nearly pure  $\text{CO}_2$  in the dry gas (Naughton et al. 1973). The average 3-year  $^4\text{He}/\text{CO}_2$  ratio was measured at  $(14 \pm 8) \times 10^{-6}$  by Naughton et al. (1973), which yields  $14 \pm 8$  ppm He. Suggestions in the data in the 1970s of short-term  $^4\text{He}$  spikes with broad correlation to synchronous volcanic events at Kilauea at that time were, perhaps, underappreciated by these early workers (see Naughton et al. 1973, their Fig. 1).

Using similar assumptions, Craig and Lupton (1976) estimated ~8.5 ppm  $^4\text{He}$  on two samples collected there in 1974. From 1982 to 1984,  $^4\text{He}$  concentrations were monitored in the New Well (drilled nearby to the Old Well site at Sulfur Banks, Fig. 1) over a 2-year period and slowly reached a maximum of 16 ppm from lows

of 6 ppm (Friedman and Reimer 1987). In 1991, calculated  $^4\text{He}$  concentrations were 4.2–4.4 ppm based upon reported He-isotope ( $R_C/R_A$ ) and  $\text{CO}_2/{}^3\text{He}$  values in duplicate samples collected from the New Well, assuming nearly pure  $\text{CO}_2$  in the dry gas (Hilton et al. 1997). (Lower  $\text{CO}_2$  concentrations in the vent gas, which were not reported, would increase the helium concentrations). In 1997, a mean dry-gas concentration of 7.2 ppm was reported for the Old Well, with maximums of 10.5 and 17.1 ppm in comparative gas samples from a gas workshop held at Kilauea (Elias 1999). From 2018 to present, quarterly monitoring of the Old Well site has reported  $^4\text{He}$  concentrations that vary from just above ambient air (5.2 ppm) to a maximum of only 6.3 ppm (Peek et al. 2020) (Fig. 9). There appears to be a long-term, decadal trend towards lower  $^4\text{He}$  concentration at Sulfur Banks.

## Discussion

### Correction for Air Contamination *in-situ* using ${}^{40}\text{Ar}$

Ideally, the fumarole gas should be pure or in need of only a small correction for air contamination (Sano and Wakita 1985; Sakamoto et al. 1992). However, when field-testing a new instrument, this situation is often not the case. The common practice in samples returned to the lab for helium isotope analysis is to measure the  $^4\text{He}/{}^{20}\text{Ne}$  ratio in the sample and compare this measurement to the known  $^4\text{He}/{}^{20}\text{Ne}$  ratio in air (e.g., Sano and Wakita 1985). Because the only known planetary reservoir for  ${}^{20}\text{Ne}$  is the atmosphere, this correction accurately estimates air contributions. Other noble gases such as  ${}^{40}\text{Ar}$ , which is radiogenic, can have mantle and crustal reservoirs, which are nevertheless comparatively small and measurable. The analytical problem for most smaller, lower resolution mass spectrometers such as the quadruples used here is isobaric interference of  ${}^{40}\text{Ar}^{++}$  with  ${}^{20}\text{Ne}^+$ , even if most  ${}^{40}\text{Ar}$  can be removed by cryogenic trapping (e.g., Sakamoto et al. 1992) and  ${}^{40}\text{Ar}^{++}$  suppressed with the use of AIMS (Adjusted Ionization Mass Spectrometry) techniques (McMurtry et al. 2019a). Here we used Ar concentrations determined in companion samples by gas chromatography as an air contamination correction, after a small correction for any mantle or volcanic contributions (McMurtry et al. 2019b). Ideally, Ar should be measured in the same sample gas as the HIM *in-situ*. Future deployments would benefit from a second mass spectrometer similar to the VGAM (McMurtry et al. 2019c) that can measure Ar in the sample chamber if the NEG-Ion pump of that instrument is replaced with a compact turbomolecular-roughing pump, as we have done previously.

### Sampling of $\text{CO}_2$ -enriched near-ground gas at Sulfur Banks

Following the field deployment of the *in-situ* instrument, the equipment was returned to the lab and He isotopes

were determined in lab air, yielding He isotope values ranging from 0.5 to 1.6  $R_A$  (average of  $1.0 \pm 0.39 R_A$ , see lab air series in Table 1), which reflect the overall precision of the method at determining air-like He isotope values. A possible explanation for the higher measured  ${}^3\text{He}/{}^4\text{He}$  in the ambient, near-ground field samples vs. lab air may be higher hydrogen pressures in the high vacuum that built up when the instrument was powered off between sampling to conserve power. Normally in the lab, the instrument's high vacuum is continuously pumped by an ion pump, which, because of its modest size and pumping speed ( $\sim 20$  L/sec), needs long exposure to effectively decrease the hydrogen (and interfering HD isobar) partial pressure.

Alternatively, the higher measured  ${}^3\text{He}/{}^4\text{He}$  in these samples may reflect a dilute plume or  ${}^3\text{He}$ -enriched near-ground gas. The ambient intake was located approximately 30 cm above the ground. Notably, this gas was not air-like, instead it had elevated  $\text{CO}_2$  concentrations that ranged from 710 to 1081 ppm and Ar values lower than air (Table 3), as well as uncorrected He isotope ratios that ranged from 3.0 to 3.8  $R_A$  (Table 1). We surmise that the variability observed in the He data results from turbulent air mixing between high  ${}^3\text{He}/{}^4\text{He}$  fumarole gas and ambient air.

The compositional gas results suggest that  $\text{CO}_2$ -enriched ground gas emanates approximately 9 m south of the Old Well site (Fig. 1d). This site is at the northern edge of a linearly distributed bare ground area, which is likely fault controlled, located within the vicinity of the 2.0 ppm total  $^4\text{He}$  anomaly (above ambient air) of Friedman and Reimer (1987) (Fig. 2c). At the Old Well, our measurements of total  $^4\text{He}$  concentration in the *in-situ* sample runs were not significantly above the ambient air mean value of 5.24 ppm (Table 1; Fig. 9), which is consistent with recent low  $^4\text{He}$  measurements of 5.4–6.3 ppm ( $n=7$ ) in Old Well vent gas (Peek et al. 2020) and with even lower  $^4\text{He}$  values measured using our conventional techniques (Table 2). The bare ground area may nevertheless be significant for  $\text{CO}_2$ -rich gas emissions, indicating an occurrence of  $\text{CO}_2$ -rich soil gas that would be poisonous to most plant life, as was also observed at Mammoth Mountain (Hurwitz et al. 2018). Follow up work should include a more direct sampling approach to the soil gas at this site.

### He isotope variability at sulfur banks

HIM sampling was conducted on a daily basis from 8 to 20 December, with one sampling day lost on 13 December (total of 12 samples collected; Table 1; Fig. 6). Daily ground-truth sampling began on 10 December and ran through 20 December, with 12 Giggenbach samples collected through 19 December and 15 copper tube samples collected for helium and isotopes (Table 2; Fig. 6). High

$^3\text{He}/^4\text{He}$  results were obtained from the Barry lab on 17 December (both VGPS exhaust and Tee) and on 20 December (both VGPS exhaust and Tee, with a comparable USGS lab result on the Tee duplicate copper tube sample, Table 2). The remainder of the WHOI dataset reports  $^3\text{He}/^4\text{He}$  results close to the air value. Earlier samples, collected at the VGPS exhaust when the HIM was collecting near-ground gas, may be accurate (commented as OK in Table 2), but the air-like results on 19 December from fumarole samples suggest a sample acquisition, storage, or extraction problem prior to introduction to the isotopic analysis, as previously discussed (see Fig. 6). A comparison of the  $\text{CO}_2$  concentrations from the companion Giggenbach samples to the WHOI isotopic results from copper tube samples in Fig. 7 suggests those additional samples that were probably lost ( $n=6$ ). In other words, the WHOI daily samples that displayed high  $^3\text{He}/^4\text{He}$  results ( $n=4$ ) are accurately reporting fumarole compositions, and those showing air-like values are suspect, as denoted in Table 2.

The apparent long-term variability of the measured He isotopes at Sulfur Banks solfatara appears minor, ranging from lows of  $13.7 R_A$  to highs of nearly  $16 R_A$  over a period of 44 years (Craig and Lupton 1976; Torgersen and Jenkins 1982; Hilton et al. 1997; McMurtry et al. 2019b; Peek et al. 2019, 2020). Another aspect of this apparent stability is whether the emanating gases at Sulfur Banks are coupled or decoupled from the shallow summit reservoir that drives the eruptions at nearby Halema'uma'u Crater and within the two major rift zones downslope, which receive magma from a deeper summit reservoir (Neal et al. 2019). We report a signal of the most recent eruption of Halema'uma'u Crater that appeared in the He isotopes at least one day prior to the eruption, which strongly suggests a connection from the shallow summit magma reservoir to the Sulfur Banks solfatara field. The air-corrected He isotope ( $R_C/R_A$ ) values indicate a jump from minimum values on December 15th sampling of  $14.7 R_A$  to values of  $16.0$  to  $17.0$  on December 20th before returning to  $14.8 R_A$  by December 31st (T. Nadeau, pers. Comm., 2021; Table 1; Fig. 6). Daily to sub-daily sampling of helium isotopes at Sulfur Banks can therefore potentially indicate an impending eruption at Kilauea that was not forecast by the extensive seismic network or other monitors, such as tilt and  $\text{CO}_2/\text{SO}_2$  ratios in the plume plus conventional fumarole gas monitoring at Kilauea (see: USGS Hawaiian Volcanoes Observatory, Volcano Awareness Month (January); <https://www.usgs.gov/center-news/volcano-awareness-month-2021-program-what-s-happening-k-lauea-volcano>). Besides increasing the sampling frequency, such instrumentation, once established and with added internal calibration standards, should eliminate many of the pitfalls of conventional He sampling and remote analysis.

### Power budget

The HIM station was drawing peak power loads of 425 W for 30 min during analysis and 380 W for one hour of subsequent glass clearing (Fig. 10). Average power draw per cycle was just over 200 W. The solar PV system used was capable of providing a combined panel output of 375 (REC™) plus 165 (Ganz™) W-hours, or 540 W-hours. The solar charging power is only available in daylight hours and was affected by increasing cloudy and rainy conditions during the deployment (Fig. 6). These conditions necessitated once-daily analysis, powering the station down between sampling, and eventual swapping of the Pb-acid batteries with units charged overnight by battery chargers. Because of the high-visibility location within a National Park, no power cabling in or fumarole gas piping out to a remote location with grid power was allowed, as was done previously at Sulfur Banks (Friedman and Reimer 1987).

Future deployments will benefit from an additional 375 W REC™ PV panel in place of the three lower-power Ganz™ PV panels (Fig. 2a). Because cloudy and rainy conditions there are inevitable, additional power could be provided from relatively quiet and compact hydrogen fuel cell generators, such as 250-W portable units made by Ultra Electronics™. Additional larger capacity batteries would also be beneficial. In terms of energy consumption, we are making improvements to the He glass membrane that will make it much smaller and thinner, perhaps increasing the He flux into the high vacuum while minimizing or even obviating the long and high-power glass cleansing step (Fig. 10).

### Final considerations

We report on a nearly two-week test deployment of the Helium Isotope Monitor (HIM; McMurtry et al. 2019a, b) station within the Sulfur Banks solfatara field on the summit of Kilauea Volcano, Hawaii. The current HIM and associated Vent Gas Purification System (VGPS) consume moderately high power at an average of over 200 W during a typical four-hour sample acquisition, which includes heating the glass to clear it of stored helium isotopes between samples. Because of the location of the Old Well sampling site in a US National Park, we were constrained to operate on batteries charged in this case by solar voltaic (PV) panels. Keeping the footprint of the station to a minimum further constrained the size of the solar PV array. For the anticipated power loads, the weather had to be mostly sunny, which was initially the case, but then deteriorated for the remainder of the deployment. The Sulfur Banks solfatara field is located on a weather divide where predominately easterly winds drive trade wind showers. Any attempt at long-term monitoring there will require supplemental power from sources such as fuel cell generators (to keep noise

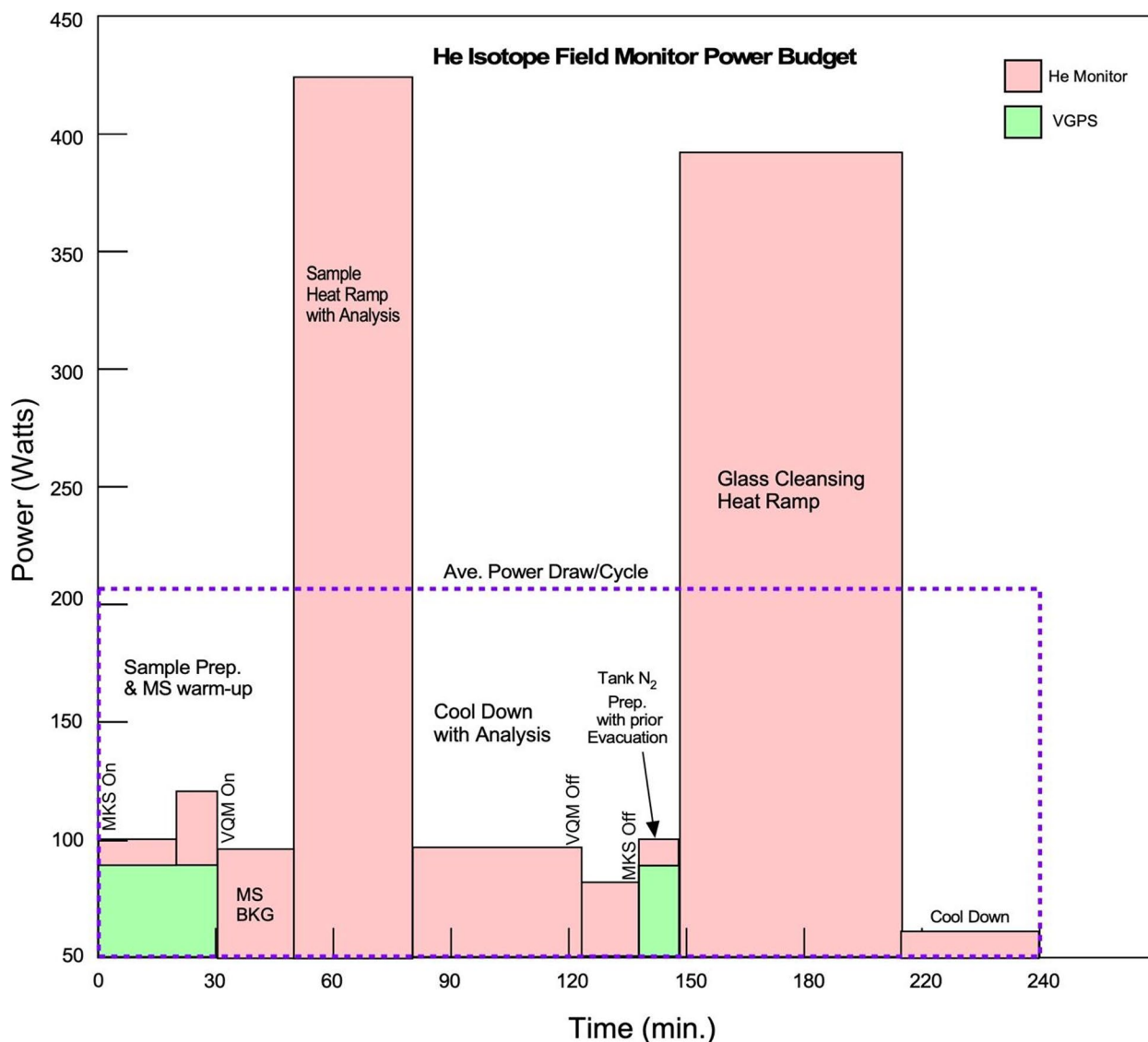


**Fig. 10** Histogram plot of measured power draw over elapsed time for the Helium Isotope Monitor (HIM) and Volcanic Gas Purification System (VGPS). The present programmed duty-cycle of ~4 h is shown. VQM=Vacuum Quality Monitor, an autoresonant ion trap mass spectrometer system; MKS=a customized high-resolution quadrupole mass spectrometer system

and other pollution to a minimum), or an agreement with the National Parks Service (NPS) to allow the provision of grid AC power to the site. To aid the power consumption issue, we are also working upon new helium sensors that will greatly reduce the power required to heat quartz glass.

A further NPS requirement was keeping the station at a distance from the Old Well sampling site, which is near a pedestrian walkway. The additional sample tubing to the station had the unforeseen positive effect of cooling the fumarole gas with ambient air and facilitating water condensation (hat tip to Jeffrey Sutton, retired from USGS HVO). We therefore abandoned the refrigeration

unit designed for this purpose and saved on its power consumption.

The Old Well site provides shallow-water saturated volcanic vent gas that is presently dominated by CO<sub>2</sub>. When compared with previous analyses done there by various researchers dating back to the late 1960s to early 1970s (Fig. 9), total <sup>4</sup>He is presently remarkably low in the dry vent gas. The long-term <sup>3</sup>He/<sup>4</sup>He variability in the summit gas appears low but there have been over 2 R<sub>A</sub> increases prior to summit activity in May 2018 (McMurtry and Dasilveira 2023, in review) and an apparent 2 R<sub>A</sub> increase over a much shorter period prior to the December 2020 eruption reported here.

Because of the power constraints on the present HIM system, we had to reduce our sampling to daily runs of vent gas and abandon planned air sampling. The air sampling can add a known standard value at low  $R/R_A$ . We plan to add a higher  $R/R_A$  internal standard that can be run at rates up to once per day.

Correction for air contamination *in-situ* is another research priority for a truly autonomous HIM system. The addition of a second MS, such as the VGAM (McMurtry et al. 2019c), to analyze the dry gas in the HIM sample chamber would allow an *in-situ* air correction using  $N_2$  and/or  $O_2$ , or measurement of  $^{40}Ar$  in a turbo-pumped version of the instrument.

#### Acknowledgements

We thank Daniel Bertin and three anonymous reviewers of a previous version of the manuscript for their comments and suggestions, which improved the presentation of this work. We thank Lopaka Lee, Tricia Nadeau, and Tamar Elias of the USGS Hawaiian Volcanoes Observatory for their able assistance in the field, and Andy Hunt of the USGS Denver isotope lab for his helpful assistance with our laboratory and field effort. This work was carried out under research permit no. HAVO-2019-SCI-0060 of the US National Parks Service. We thank Rhonda Loh and David Benitez of the NPS Hawaiian Volcanoes National Park for their abiding support of this work. James Jolly of the SOEST Engineering Support facility provided valuable electrical engineering. Philip Rapoza of SOEST PPSF provided able help with the station logistics. We thank James Blessing and MKS Instruments, Inc. for their ongoing support. Tobias Fischer of UNM provided valuable gas chemical analyses and Peter Barry of the WHOI isotope lab provided He isotopic data in support of our field effort. David V. Bekaert of Centre for Petrographic and Geochemical Research (CRPG) helped us with the production of Fig. 1. The late David R. Hilton was always an interested and able field and lab partner in elucidating the systematics of the Hawaiian plume, using *in-situ* monitoring and isotopic tools. He was there from the start of this research, and his spirit remains to guide and inspire us. This is SOEST Contribution no. 11703.

#### Author contributions

G. M. M. was project leader and designed the HIM instrument and the field test program. L. A. D. assisted in the design and testing of the HIM instrument and assisted in the field test program. Both authors contributed to writing of the manuscript.

#### Funding

The Helium Isotope Monitor was produced with support from the US Geological Survey through an Innovation Center award to Gary McMurtry and Shaul Hurwitz.

#### Data Availability

All materials described in the manuscript, including all relevant raw data, will be freely available to any scientist wishing to use them for non-commercial purposes, without breaching participant confidentiality. Contacts are: Gary M. McMurtry, mcmurtry@hawaii.edu; Luis A. Dasilveira, luis@hawaii.edu.

#### Declarations

##### Competing interests

Gary M. McMurtry reports writing assistance was provided by University of Hawai'i at Manoa. Gary M. McMurtry reports a relationship with University of Hawai'i at Manoa that includes: Gary M. McMurtry has patent #US10,005,033 B2, "Isotopic enrichment of helium-3 through glass" issued to Pacific Environmental Technologies, LLC.

##### Ethics approval and consent to participate

Not applicable.

##### Consent for publication

Not applicable.

Received: 8 November 2022 / Accepted: 2 July 2023

Published online: 02 August 2023

#### References

- Aiuppa A, Fischer TP, Plank T, Robidoux P, Di Napoli R (2017) Along-arc, inter-arc, and arc-to-arc variations in volcanic gas  $CO_2/S_T$  ratios reveal dual source of carbon in arc volcanism. *Earth Sci Rev* 168:24–47
- Allen ET (1922) Preliminary tests of the gases at Sulphur Banks, Hawaii, Monthly Bulletin of the Hawaii Volcano Observatory, Vol. X, No. 8
- Barry PH, De Moor JM, Chiodi A et al (2022) The helium and carbon isotope characteristics of the Andean Convergent Margin. *Front Earth Sci* 10. <https://doi.org/10.3389/feart.2022.897267>
- Craig H, Lupton JE (1976) Primordial neon, helium, and hydrogen in oceanic basalts. *Earth Planet Sci Lett* 31:369–385
- Davies S, Rees JA, Seymour DL (2014) Threshold ionisation mass spectrometry (TIMS); a complementary quantitative technique to conventional mass resolved mass spectrometry. *Vacuum* 101:416–422
- Elias T (1999) Preliminary evaluation of the 6th workshop results, in IAVCEI Sixth Field Workshop on Volcanic Gases, Commission on the Chemistry of Volcanic Gases, Newsletter no. 14, July 1999, 20 pp
- Friedman I, Reimer M (1987) Helium at Kilauea Volcano, Part 1, Spatial and temporal variations at Sulphur Bank, in Volcanism in Hawaii. U. S. Geological Survey Prof. Paper 1350, Chapt. 33, 809–813
- Goff F, McMurtry GM (2000) Tritium and stable isotopes of magmatic waters. *J Volcanol Geotherm Res* 97:347–396. [https://doi.org/10.1016/S0377-0273\(99\)00177-8](https://doi.org/10.1016/S0377-0273(99)00177-8)
- Hilton DR, McMurtry GM, Kreulen R (1997) Evidence for extensive degassing of the hawaiian mantle plume from helium-carbon relationships at Kilauea Volcano. *Geophys Res Lett* 24:3065–3068
- Hunt AG (2015) Noble Gas Laboratory's standard operating procedures for the measurement of dissolved gas in water samples, U.S. Geological Survey Techniques and Methods, book 5, chap. A11. <https://doi.org/10.3133/tm5A11>
- Hurwitz S, Peek S, Kelly PJ, Lewicki JL, Bergfeld D, Evans W, Wilkinson SK, Hunt AG, McMurtry GM, Jolly J, Deluze J, Horn E, Lucic G, Oze C, Horton TW (2018) New technologies to measure temporal variations of magmatic helium and  $CO_2$  emissions at Mammoth Mountain California, American Geophysical Union, Fall Meeting 2018, abstract #V43I-0251.
- Lee H, Fischer TP, Muirhead JD, Ebinger CJ, Kattenhorn SA, Sharp ZD, Kianji G, Naoto T, Sano Y (2017) Incipient rifting accompanied by the release of subcontinental lithospheric mantle volatiles in the Magadi and Natron basin, East Africa. *J Volcanol Geotherm Res* 346:118–133
- Lespez L, Lescure S, Saulnier-Copard S et al (2021) Discovery of a tsunami deposit from the bronze age Santorini eruption at Malia (Crete): impact, chronology, extension. *Sci Rep* 11:15487. <https://doi.org/10.1038/s41598-021-94859-1>
- Masuda J et al (2002) The  $^3He/^4He$  ratio of the new internal He Standard of Japan (HESJ). *Geochem J* 36:191–195
- McMurtry GM, Dasilveira LA (2023) Helium isotopes constrain magma sources and emplacement beneath Kilauea caldera during the 2018 and 2020 eruptions. *Chem Geol* (in review).
- McMurtry GM, DeLuze JR, Hilton DR, Blessing JE (2019a) Differential diffusion of helium isotopes in glass, quantum-tunneling  $^3He$  enrichment, and portable  $^3He/^4He$  monitoring of mantle processes. *Sci Rep* 9:5213. <https://doi.org/10.1038/s41598-019-41360-5>
- McMurtry GM, Dasilveira LA, Horn EL, DeLuze JR, Blessing JE (2019b) High  $^3He/^4He$  ratios in lower East Rift Zone steaming vents precede a new phase of Kilauea 2018 eruption by 8 months. *Sci Rep* 9:11860. <https://doi.org/10.1038/s41598-019-48268-0>
- McMurtry GM, Dasilveira LA, Falinski KA, Fischer TP (2019c) VGAM: Compact and low power mass spectrometer-based instrumentation for volcanic gas monitoring. *Geochem Geophys Geosyst* 20:3782–3798
- National Academies of Sciences, Engineering, and Medicine (2017) Volcanic eruptions and their repose, Unrest, Precursors, and timing. The National Academies Press, Washington, DC. <https://doi.org/10.17226/24650>
- Naughton JJ, Lee JH, Keeling D, Finlayson JB, Dority G (1973) Helium flux from the Earth's Mantle as estimated from hawaiian fumarolic degassing. *Science* 180:55–57
- Neal CA et al (2019) The 2018 rift eruption and summit collapse of Kilauea Volcano. *Science* 363:367–374

- Padrón E, Pérez NM, Hernández PA, Sumino H, Melián GV, Barrancos J, Nolasco D, Padilla G, Dionis S, Rodríguez F, Hernández I, Calvo D, Peraza MD, Nagao K (2013) Diffusive helium emissions as a precursory sign of volcanic unrest. *Geology* 41:539–542
- Paonita A, Caracausi A, Martelli M, Rizzo AL (2016) Temporal variations of helium isotopes in volcanic gases quantify pre-eruptive refill and pressurization in magma reservoirs: The Mount Etna case. *Geology* 44:499–502
- Peek S, Hurwitz S, Elias T, Nadeau PA, Hunt AG (2019) Helium isotope and gas chemistry variations at Sulphur Banks, Kilauea Volcano, HI, American Geophysical Union, Fall Meeting 2019, abstract #V31H-0094
- Peek SE, Nadeau PA, Warren SM, Elias T, Hunt AG, Hurwitz S (2020) Gas chemistry and isotope compositions at Sulphur Banks, Kilauea Volcano, Hawaii: U.S. Geological Survey data release. <https://doi.org/10.5066/P9V9FSFZ>
- Sakamoto M, Sano Y, Wakita H (1992) He/<sup>4</sup>He ratio distribution in and around the Hakone volcano. *Geochem J* 3:189–195
- Sano Y, Wakita H (1985) Geographic distribution of <sup>3</sup>He/<sup>4</sup>He ratios in Japan: implications for arc tectonics and incipient magmatism. *J Geophys Res* 90:8729–8741
- Sano Y, Wakita H (1988) Helium isotope ratio and heat discharge rate in Hokkaido island, northeastern Japan. *Geochem J* 22:293–303
- Sano Y, Nakamura Y, Wakita H, Urabe A, Tominaga T (1984) Helium-3 emission related to volcanic activity. *Science* 224:150–151
- Sano Y, Nakamura Y, Notsu K, Wakita H (1988) Influence of volcanic eruptions on helium isotope ratios in hydrothermal systems. *Geochim Cosmochim Acta* 52:1305–1308
- Sano Y, Gamo T, Notsu K, Wakita H (1995) Secular variations of carbon and helium isotopes at Izu-Oshima volcano, Japan. *J Volcanol Geotherm Res* 64:83–94
- Sano Y, Kagoshima T, Takahata N, Nishio Y, Rouleau E, Pinti DL, Fischer TP (2015) Ten-year helium anomaly prior to the 2014 Mt Ontake eruption. *Sci Rep* 5:13069. <https://doi.org/10.1038/srep13069>
- Sorey ML, Kennedy BM, Evans WC, Farrar CD, Suemnicht GA (1993) Helium isotope and gas discharge variations associated with crustal unrest in Long Valley Caldera, California, 1989–1992. *J Geophys Res* 98:15871–15889.
- Torgersen T, Jenkins WJ (1982) Helium isotopes in geothermal systems: Iceland, the geysers, raft river and Steamboat Springs. *Geochim Cosmochim Acta* 46:739–748
- Wilkes TC, Pering TD, Aguilera F et al (2023) A new permanent, low-cost, low-power SO<sub>2</sub> camera for continuous measurement of volcanic emissions. *Front Earth Sci* 11–2023. <https://doi.org/10.3389/feart.2023.1088992>
- Winchester S (2004) *Krakatoa: the day the world exploded*, August 27, 1883. Harper-Collins, New York

### Publisher's Note

Springer Nature remains neutral with regard to jurisdictional claims in published maps and institutional affiliations.